PRAMANA
— journal of
physics

Vol. 65, No. 6
December 2005
pp. 1041–1051

Structure of high spin states of ^{76}Kr and ^{78}Kr nuclei

U R JAKHAR[1], H L YADAV[1] and A ANSARI[2]
[1]Department of Physics, Rajasthan University, Jaipur 302 004, India
[2]Institute of Physics, Sachivalaya Marg, Bhubaneswar 751 005, India
E-mail: ansari@iopb.res.in

MS received 11 April 2005; revised 8 August 2005; accepted 20 August 2005

Abstract. Following a fully self-consistent cranked Hartree–Fock–Bogoliubov (CHFB) approach with a pairing+quadrupole+hexadecapole model interaction Hamiltonian the structure of the yrast states of ^{76,78}Kr nuclei is studied up to angular momentum $J = 24$. Evolution of the shape with spin, and rotation alignment of proton as well as neutron $0g_{9/2}$ orbitals is investigated along with the inter- and intra-nucleus variations of the g factors as a function of J. We find that the shape of ^{78}Kr remains prolate all through up to $J = 24$, whereas ^{76}Kr becomes triaxial beyond $J = 12$.

Keywords. Kr nuclei; high spin states; g-factors; cranked Hartree–Fock–Bogoliubov theory.

PACS Nos 27.50.+e; 21.10.-k; 21.10.Hw

1. Introduction

An exhaustive study of high spin states in ^{76,78}Kr nuclei was carried out experimentally as well as theoretically in as early as 1989 by Gross *et al* [1]. The yrast levels were extended up to $J = 24$. The kinetic moment of inertia ($\sim J/\omega$, with $\omega = (E_J - E_{J-2})/2$) is found to show strong variations as a function of the rotational frequency, ω. In ref. [1] the band crossings and single particle (sp) angular momentum alignments are analysed in the cranked shell model approach [2]. It is found that alignments of pairs of protons and neutrons in $0g_{9/2}$ orbitals play a significant role, with proton pairs aligning first. Pairing correlation is considered only between the like particles. The lifetime measurements in ^{76}Kr indicate that the quadrupole deformation parameter β remains almost constant up to spin 10^+ with a value of about 0.33. The oblate minimum is found to lie only about 600 keV higher than the prolate one for the ground state of ^{76}Kr, leading to γ-softness and shape coexistence in ^{76,78}Kr. In earlier papers [3,4] it has been concluded that in ^{76}Kr the pronounced band crossing is caused by a simultaneous alignment of neutrons and protons both in $0g_{9/2}$ orbitals leading to an aligned sp angular momentum $i_x = \langle j_x \rangle \approx 7.0$ (in units of $\hbar$). Similar conclusion is reached by Algora

et al [5] regarding ^{74}Kr in a deformed Woods–Saxon + Strutinsky calculation with $\beta = 0.43$ and $\beta_4 = 0.005$ in the ground state. For ^{78}Kr [6] the experimental data show two small upbends, the first one is relatively more pronounced at $J = 10$–12 with $i_x \approx 3$, while the second one occurs at $J = 18$. These upbends are expected to be due to the alignments of proton and neutron pairs, respectively in the $0g_{9/2}$ orbitals. The delayed alignment of neutrons is understandably due to the addition of two neutrons in the $0g_{9/2}$ orbitals as compared to the ^{76}Kr isotope. For a given high-j orbital and prolate deformation the alignment is most effective if only two particles near the Fermi level occupy such an orbital. Addition of more particles fill up $m > 1/2$ magnetic quantum number states, and delay/hinder alignment, though at the same time changes in self-consistent shape parameters can affect it to some extent. In fact, in ref. [7] the measurement of g factors at high spins indicates that an average value of g ($J = 8$) is about 60% of g ($J = 2$) and is interpreted as a strong indication that the first crossing in ^{78}Kr is due to a neutron alignment. Around this spin the average shape is found to be oblate in an HFB calculation.

In all these calculations discussed so far, pairing is considered only between like particles. This is consistent with recent findings of Satula and Wyss [8] that n–p pairing decreases rapidly when moving away from the $N = Z$ line (see also, ref. [9]).

After recent measurements, data are available also on rotational g factors, though not up to high spins, for $^{76-82}$Kr isotopes [10–12]. These can play decisive role to test various model calculations, as is already apparent from the above discussions about ^{78}Kr. Over the years there have been several theoretical calculations to study the structure of Kr isotopes, in the ground state as well as at finite spins [1,2]. However, none is fully self-consistent in all the shape degrees of freedom of an effective Hamiltonian. So, we have chosen to further investigate the high spin properties of these nuclei following a fully self-consistent CHFB method employing a pairing+quadrupole+hexadecapole model interaction with cranking about the x-axis [13–15]. For the present calculation we have chosen only ^{76}Kr and ^{78}Kr, as the heavier ones become gradually spherical with neutron number approaching 50, and lighter ones require treatment of n–p pairing.

In such calculations, including shell model with the assumption of an inert core, the input of basis spherical single particle energies plays a vital role. It appears that the conflicting predictions from different model calculations are, at least partly, due to the use of different sets of basis sp energies. This aspect is investigated by studying ground state properties of ^{76,78}Kr by employing two sets of basis sp energies.

In the next section we give an outline of the formalism. Then in §3 our results will be presented and discussed. Finally in §4 summary and conclusions of these studies are presented.

2. Formalism

In what follows we briefly describe the Hamiltonian and the basis space employed for the numerical calculations carried out for the ^{76,78}Kr nuclei with the assumption of an inert core made of proton number, $Z = 20$ and neutron number, $N = 20$ (i.e.

^{40}Ca). The quadrupole + hexadecapole + pairing model interaction Hamiltonian is given by

$$H = H_0 - \frac{1}{2}\sum_{\lambda=2,4}\chi_\lambda \sum_\mu \hat{Q}_{\lambda\mu}(-1)^\mu \hat{Q}_{\lambda-\mu} - \frac{1}{4}\sum_{\tau=p,n} G_\tau \hat{P}^\dagger_\tau \hat{P}_\tau \,, \tag{1}$$

where H_0 stands for the one-body spherical part, χ_λ term represents the quadrupole and hexadecapole parts with $\lambda = 2$, 4 and the G_τ term represents the proton and neutron monopole pairing interaction. Explicitly we have

$$\hat{Q}_{\lambda\mu} = \left(\frac{r^2}{b^2}\right) Y_{\lambda\mu}(\theta,\phi)\,, \tag{2}$$

$$\hat{P}^\dagger_\tau = \sum_{\alpha_\tau,\bar{\alpha}_\tau} c^\dagger_{\alpha_\tau} c^\dagger_{\bar{\alpha}_\tau}\,. \tag{3}$$

In the above equation $c^\dagger$ are the creation operators with $\alpha \equiv (n_\alpha l_\alpha j_\alpha m_\alpha)$ as the spherical basis states quantum numbers with $\bar{\alpha}$ denoting the conjugate time-reversed orbital. The standard mean field CHFB equations [16] with cranking about the x-axis are solved self-consistently for the quadrupole, hexadecapole and pairing gap parameters. The deformation parameters and pairing gaps are defined in terms of the following expectation values:

$$D_{2\mu} = \chi_2\langle\hat{Q}_{2\mu}\rangle, \quad D_{4\mu} = \chi_4\langle\hat{Q}_{4\mu}\rangle, \tag{4}$$

$$\hbar\omega\beta\cos\gamma = D_{20}, \quad \hbar\omega\beta\sin\gamma = \sqrt{2}D_{22}, \quad \hbar\omega\beta_{40} = D_{40}, \tag{5}$$

$$\Delta_\tau = \frac{1}{2}G_\tau\langle\hat{P}_\tau\rangle. \tag{6}$$

As usual, in the CHFB approach, the particle number and angular momentum are conserved on the average:

$$\langle\mathrm{CHFB}|\hat{N}|\mathrm{CHFB}\rangle = N\,, \tag{7}$$

$$\langle\mathrm{CHFB}|\hat{J}_x|\mathrm{CHFB}\rangle = \sqrt{J(J+1)}, \tag{8}$$

where $\hat{N}$ is the particle number operator and $\hat{J}_x$ is the x-component of the total angular momentum operator. The oscillator frequency $\hbar\omega = 41.0A^{-1/3}$ (MeV), and β, γ and β_{40} are the deformation parameters, while Δ_p and Δ_n are the pairing gap parameters for protons and neutrons, respectively. The basis space consists of $N = 3, 4$ major shells + $0h_{11/2}$ orbitals for protons, as well as for neutrons. The spherical single particle energies for $N = 3$ fp-shell + $0g_{9/2}$ orbitals are taken from ref. [18] where microscopic aspects of shape coexistence and shape transitions have been studied for ^{72,74}Kr nuclei. The energies of the remaining orbitals are adjusted with respect to these levels following roughly the spherical Nilsson model energies

Table 1. Basis single particle oscillator orbitals and their energies in units of $\hbar\omega = 41/A^{1/3}$ MeV for protons as well as neutrons. The numbers under column A (set A) represent the ones used in most of the present calculations, and those under column B (set B) give the spherical Nilsson model energies [19], which are also employed for part of the calculations.

Orbitals	A		B	
nlj	ϵ_j^p	ϵ_j^n	ϵ_j^p	ϵ_j^n
$1p_{1/2}$	0.040	−0.070	0.0000	0.0000
$1p_{3/2}$	−0.270	−0.332	−0.2102	−0.1916
$0f_{5/2}$	0.300	0.130	−0.2435	−0.2046
$0f_{7/2}$	−0.560	−0.690	−0.7338	−0.6518
$0h_{11/2}$	1.088	1.018	0.8575	0.9877
$2s_{1/2}$	0.987	0.831	1.1284	1.1049
$1d_{3/2}$	1.072	0.879	1.1084	1.0971
$1d_{5/2}$	0.557	0.479	0.7581	0.7777
$0g_{7/2}$	0.662	0.591	0.7115	0.7595
$0g_{9/2}$	0.029	−0.043	0.0810	0.1846

[19]. Such single particle energies ϵ_j are listed in table 2. in units of $\hbar\omega = 41/A^{1/3}$ under column A, and we term them as set A. In the same table the second set of sp energies (set B) are the spherical Nilsson model energies which are also used in some part of the calculations to be discussed later on. As discussed in ref. [17], the upper shell radial matrix elements are reduced by the factors $(N_0+3/2)/(N+3/2)$, where N_0 takes the value 3 in the present case. Finally the interaction strengths are chosen such that reasonable values of the ground state shape parameters, and the first 2^+ excitation energies are obtained. The pairing interaction strengths ($G_{p,n}$) are chosen such that in the ground state the value of the pairing gap is approximately 80% of the odd–even mass difference [20]. The following values of the interaction strengths (all in MeV) are chosen:

$$\chi_2 = 64/A^{1.4}, \quad \chi_4 = 50/A^{1.4}, \quad G_p = 18.5/A, \quad G_n = 18.0/A. \tag{9}$$

3. Results and discussion

In the CHFB theory the number of particles and angular momenta are conserved only on the average (eqs (7) and (8)) and these are well-known limitations of this approach. On the other hand, this has the advantage of being approximately a variation after angular momentum projection method as the variation is performed for each value of the angular momentum. Also the features of alignment of sp angular momenta along the axis of rotation are inherently present in this model. In this light we would like to discuss our results for ^{76,78}Kr isotopes.

Table 2. Intrinsic ground state shape parameters along with the excitation energy E_2 corresponding to the prolate shape solution and the intrinsic energy difference between the prolate and oblate minima, $\delta E_{\mathrm{P-O}}$ for ^{76,78}Kr.

Nucleus	β	β_{40}	Δ_p (MeV)	Δ_n (MeV)	E_2 (MeV)	$\delta E_{\mathrm{P-O}}$ (MeV)
^{76}Kr	0.345	0.024	1.017	0.846	0.243	–
	−0.165	0.005	1.274	1.479	–	−2.500
^{78}Kr	0.323	0.017	1.001	1.062	0.264	–
	−0.145	0.003	1.243	1.433	–	−1.416

In table 2 we list the shape parameters for the ground state. We have looked for the axial prolate ($\gamma = 0$) as well as oblate ($\gamma = 180°$) solutions to check for the coexistence of these shapes in these nuclei. As listed in the table, the energy difference between the prolate and oblate minima, $\delta E_{\mathrm{P-O}}$ comes out to be −2.5 MeV and −1.416 MeV, respectively for ^{76}Kr and ^{78}Kr, which indicates that the ground state shape is a good prolate one. When the energies corresponding to these minima are compared with respect to the spherical shape solutions, the oblate minima are found to be lower with respect to these only by 337 keV and 230 keV, respectively for ^{76}Kr and ^{78}Kr. Thus, it further indicates that the oblate minima would be rather unstable with respect to fluctuations like zero point motion etc.

The experimental value of the energy of the first excited 2^+ state is 424 keV and 455 keV for ^{76}Kr and ^{78}Kr, respectively, with the corresponding calculated numbers being 243 keV and 264 keV. The smaller calculated numbers are desirable because these will increase if angular momentum and particle number projections are carried out. These are the reasons to choose pairing gaps as about 80% of the empirical values from odd–even mass differences [20]. We notice that experimental as well as theoretical values for the heavier isotope are slightly larger. Somewhat consistent with the values of β, we get the ratio $R_4 = E_4/E_2 = 3.05$ and 2.78 for ^{76}Kr and ^{78}Kr, respectively which are 2.44 and 2.46 (almost same) from the experimental data. Now we present in figure 1 the values of the deformation parameters as a function of J for both the isotopes. The curves with open triangles ($\triangle$) are for ^{76}Kr while the ones with open circles ($\circ$) are for ^{78}Kr. For the former isotope the values of β are in good agreement with the experimental ones up to $J = 10$. It may be noticed that in the ground state the values of β as well as β_4 for ^{78}Kr are smaller than that for ^{76}Kr. But beyond $J = 4$, the trend gets reversed. At the highest spin ($J = 24$) considered, ^{76}Kr becomes very soft leading to a triaxial shape with $\gamma \approx 20°$, whereas ^{78}Kr remains a well-deformed prolate. This is in contradiction to the earlier model calculations [1,6], but very much consistent with the experimental data on moment of inertia ($\mathcal{I} = (2J-1)/E_\gamma^J$) [4].

In figure 2 are displayed the variation of the pairing gaps Δ_p and Δ_n for the protons and neutrons, respectively. It is seen that with the increase of spin the neutron pairing collapses very rapidly already at $J = 6$ for both the isotopes, though it is quite sizeable in the ground state. Contrary to this, the proton pairing persists for much higher spin values in both the nuclei considered. In a particle number projected approach this should become much more stable, thus quite appropriate to term these features as the coexistence of superfluidity and rigid rotation [4].

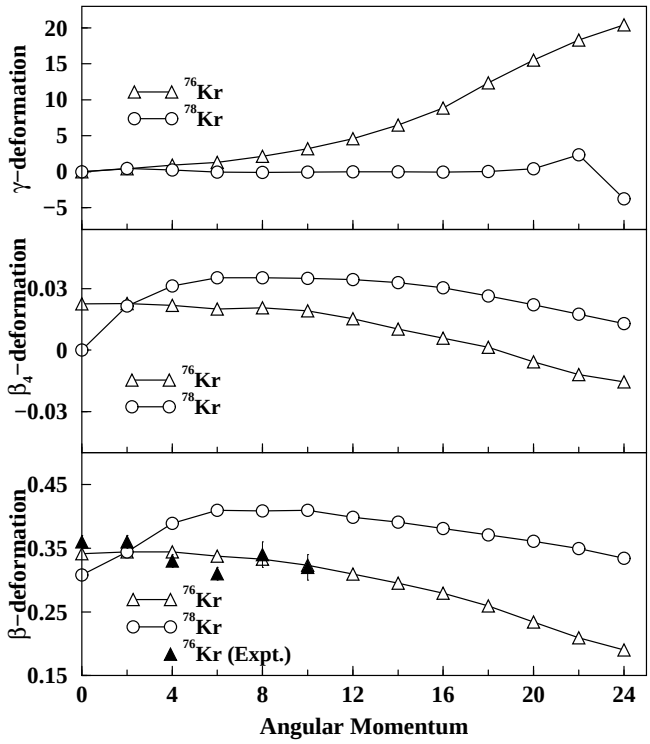

Figure 1. Intrinsic deformation parameters as a function of angular momentum of the yrast states in ^{76,78}Kr.

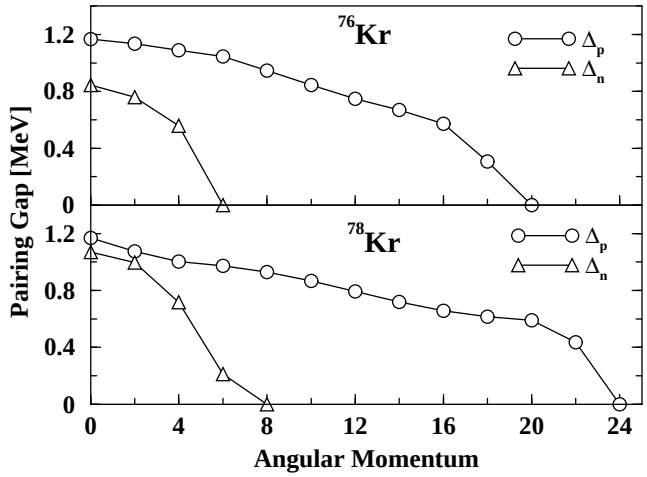

Figure 2. Dependence of proton and neutron pairing gaps on angular momentum for ^{76,78}Kr.

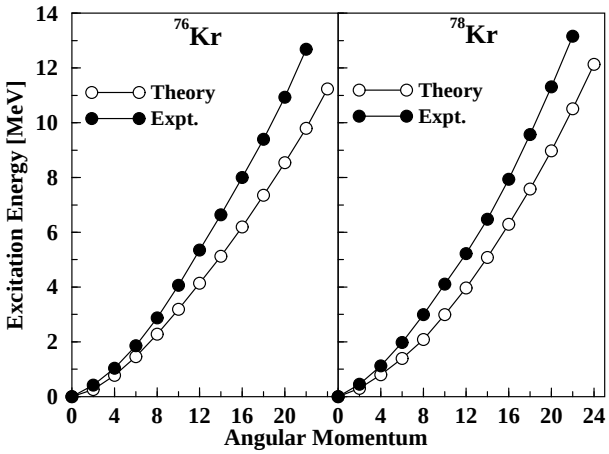

Figure 3. Energies of the yrast states of ^{76,78}Kr nuclei compared with the experimental values.

With the above dependence of the shape parameters on the average spin, we check for the energies of the yrast levels as compared to the experimental values. This is displayed in figure 3. The parabolic shape is quite well reproduced, but calculated numbers are smaller as compared to the experimental values implying larger theoretical values of the moments of inertia for both the nuclei. Usually particle number projection lowers the energy for the ground state ($J = 0$) much more than that for the excited states ($J > 0$) and this would improve the agreement.

In order to demonstrate the change in structure as a function of angular momentum, one chooses to plot (i) J vs. ω, (ii) $\mathcal{I}$ vs. J or (iii) $\mathcal{I}$ vs ω, and look for deviations from the normal $J = \omega\mathcal{I}$ type of relation. We choose the first one, as this involves a direct comparison of the two physical observables J and gamma energy, $E_\gamma^J = E_J - E_{J-2} = 2\omega_J$. The moment of inertia is a derived quantity from these two discrete variables. Plots of all the three types mentioned above are important to focus on different aspects, but we do not want to go into these details here. Regarding the definition of ω it may be added that the above relation is used for the experimental data and in theory it is just the Lagrange multiplier to the angular momentum constraint operator $\hat{J}_x$ in x-axis cranking, as is the case here. Now in figure 4 we display a plot of J vs. ω depicting the variation of the moment of inertia ($J = \omega\mathcal{I}$). Here the moment of inertia is the slope of the J–ω curve at a given value of ω. For both the nuclei, the experimental results exhibit upbends at $J \approx 12$, the upbend seen in the results for ^{78}Kr being like a sharp discontinuity at a point. In the theoretical curve this small sudden jump is smoothed out, but it does exhibit the gross features similar to the measurements. Particularly the average slope of the two parts, $J = 2$–10 and $J = 12$–22, in the experimental curve is approximately the same, and this is consistent with the prolate shape and almost a constant value of β as obtained in the present calculations. Theoretical results for ^{76}Kr show alignment features similar to the experimental ones albeit shifted at smaller frequencies. It is clear that in ^{76}Kr the change in structure at high spins is

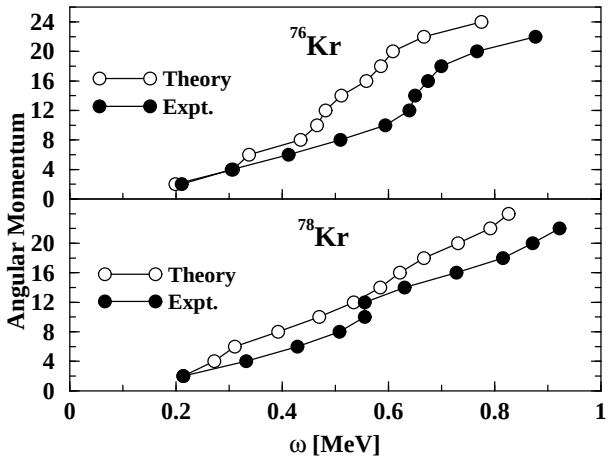

Figure 4. A plot of angular momentum vs. rotational frequency.

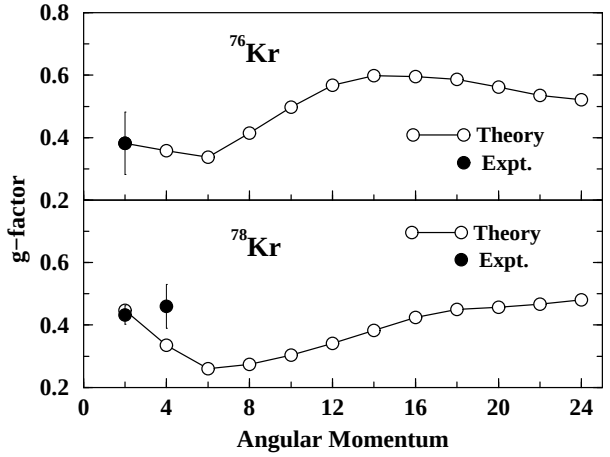

Figure 5. Variation of g factor as a function of angular momentum.

more complex than in ^{78}Kr. This is again in line with the shape changes seen from figures 1 and 2.

Next we present in figure 5 our results on rotational g factors, which are computed as $\langle\hat{\mu}_x\rangle/\langle\hat{J}_x\rangle$ for a given value of J with $\hat{\mu}_x$ being the x-component of the dipole magnetic moment operator. The values of the free single particle spin g factors are attenuated by a factor of 0.6 [14]. The experimental values are available only at $J = 2$ for ^{76}Kr and at $J = 2$ and 4 for ^{78}Kr [10,11], which are consistent with a constant value of about Z/A. Without any adjustable free parameters the theoretical value agrees with the experimental one at $J = 2$, quite well. As seen in figure 6, soon after $J = 2$ the simultaneous alignment of neutron and proton pairs in $0g_{9/2}$ starts competing with each other. In the low spin part the neutron alignment dominates, which gets reversed at high spins. As a result, the calculated

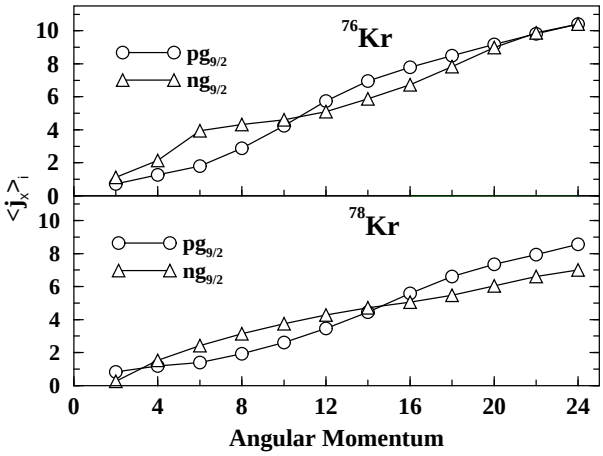

Figure 6. Contributions of protons and neutrons in $0g_{9/2}$ orbitals to total angular momenta.

value of g factor at $J = 4$ is slightly smaller than the experimental one. The decreased value at $J = 6$ seems to support the findings of ref. [7], that g factor at $J = 8$ is about 60% of that at $J = 2$. From this plot we also see that bulk of the total angular momentum is contributed by protons and neutrons in the $0g_{9/2}$ orbitals alone. Normally the alignment is stronger when there is a rapid pairing collapse. If the particle number projection is carried out, one can expect that the neutron pairing collapse will become gradual leading to slower neutron alignment and consequently somewhat larger value of g factor around $J = 4$ and 6.

3.1 *Effect of basis single-particle energies*

In a mean-field calculation with the assumption of an inert core, an appropriate choice of the basis sp energies always plays a crucial role. The spherical Nilsson sp energies [19] are often used for this purpose, as these are easily calculable with mass number dependent Nilsson parameters. Therefore, in this section we want to employ such sp energies (set B in table 1) and compare the resultant ground state properties of these nuclei *vis-à-vis* those already discussed above.

First of all with the use of these Nilsson sp energies and the interaction strengths presented in eq. (9) the ground state shape of both the nuclei turns out to be spherical. So, to obtain a deformed solution we have readjusted the interaction strength parameters to the following new values (not very precisely adjusted to produce exactly the same values of the shape parameters as in table 2):

$$\chi_2 = 74/A^{1.4}, \quad \chi_4 = 70/A^{1.4}, \quad G_p = 20.5/A, \quad G_n = 18.0/A. \tag{10}$$

The new self-consistent shape parameters obtained are presented in table 3. We notice that for ^{76}Kr the energy difference $\delta E_{\mathrm{P-O}} = -1.495$ MeV whereas for ^{78}Kr it becomes 0.255 MeV implying that oblate minimum becomes lower by about 250

Table 3. Intrinsic shape parameters in the ground state along with the energy difference between prolate and oblate minima, $\delta E_{\mathrm{P-O}}$ for ^{76,78}Kr with the use of spherical sp energies from the Nilsson model (set B in table 1).

Nucleus	β	β_{40}	Δ_p (MeV)	Δ_n (MeV)	$\delta E_{\mathrm{P-O}}$ (MeV)
^{76}Kr	0.521	0.035	1.025	0.667	–
	−0.271	0.011	1.259	0.891	−1.495
^{78}Kr	0.380	0.001	1.039	0.998	–
	−0.254	−0.010	1.276	0.837	+0.255

keV compared to the prolate one for the latter nucleus. Here one may also say to some extent that the prolate and oblate shapes coexist for ^{78}Kr in the ground state. Thus, using a pairing + quadrupole type of Hamiltonian with different sets of basis sp energies (not chosen arbitrarily) contradictory results for the ground state shape of ^{78}Kr have been obtained.

4. Summary and conclusions

We have performed a fully self-consistent cranked HFB calculation for ^{76}Kr and ^{78}Kr isotopes with $N - Z \geq 4$ and the neutron numbers not quite close to the magic number 50. Therefore, pairing correlations are important for protons as well as neutrons, and at the same time we need not incorporate the n–p pairing which is important for $N \sim Z$ nuclei. Whereas the neutron pairing collapses by $J = 6$, the proton pairing vanishes only at about $J = 24$. Such a drastic difference in the behaviour of neutron and proton pairing as a function of spin for Kr isotopes, to our knowledge, is being reported for the first time. With the present choice of the Hamiltonian parameters (eq. (9)) ^{76}Kr becomes triaxial at high spins, whereas ^{78}Kr remains a good axial rotor up to $J = 24$ with proton pairing persisting all through. We do not find the coexistence of triaxial and oblate shapes with the use of set A spherical sp energies. The angular momentum vs. rotational frequency plot shows a good qualitative agreement between theory and experiment and we conclude that change in structure with spin is qualitatively correctly described in this microscopic many-body approach.

For ^{76}Kr as well as ^{78}Kr the experimental value of g_2 is well reproduced in our calculation. Variation of the g factors as well as the rotation alignment of $0g_{9/2}$ orbitals as a function of spin shows that the alignment of neutron orbitals dominates over the proton orbitals in the low spin region. At high spins it goes the other way. However, all through there is a simultaneous alignment of neutrons as well as protons, unlike in case of rare earth backbenders (e.g. $^{156-164}$Er isotopes).

In view of the rapid collapse of neutron pairing, somewhat excessive alignment of neutron $0g_{9/2}$ orbitals at low spins, and large values of effective moment of inertia (compared to experimental values), which are all inter-related, it seems that inclusion of quadrupole pairing, and perhaps, more importantly, incorporation of the particle number projection in the CHFB code is essential to obtain better quantitative results in this approach. Our next effort will be in this direction.

We have also demonstrated that proper choice of spherical sp energies is important in such calculations, which can best be justified by comparison with the experimental data. From our results discussed above it seems that the set A sp energies listed in table 1 [18] are relatively more suitable for the study of Kr isotopes. For a more general validity in the mass region $A = 70$–80 one needs to study some more nuclei in this region.

Acknowledgments

We are grateful to the Department of Science and Technology (DST), Government of India for financial support under the project No. SP/S2/K-28/97.

References

[1] C J Gross *et al*, *Nucl. Phys.* **A501**, 367 (1989)
[2] R Bengtssn and S Frauendorf, *Nucl. Phys.* **A327**, 139 (1979)
[3] C J Gross *et al*, *Z. Physik* **A331**, 361 (1988)
[4] M S Kaplan *et al*, *Phys. Lett.* **B215**, 251 (1988)
[5] A Algora *et al*, *Phys. Rev.* **C61**, 031303R (2000)
[6] H Sun *et al*, *Phys. Rev.* **C59**, 655 (1999)
[7] J Billowes *et al*, *Phys. Rev.* **C47**, R917 (1993)
[8] W Satula and R Wyss, *Phys. Lett.* **B393**, 1 (1997)
[9] D Rudolf *et al*, *Phys. Rev.* **C56**, 98 (1997)
[10] G Kumbartzki *et al*, *Phys. Lett.* **B591**, 213 (2004)
[11] T J Mertzimekis *et al*, *Phys. Rev.* **C64**, 024314 (2001)
[12] T J Mertzimekis, A E Stuchbery, N Benczer-Koller and M J Taylor, *Phys. Rev.* **C68**, 054304 (2003)
[13] A Faessler, K R S Devi, F Grümmer, K W Schmid and R R Hilton, *Nucl. Phys.* **A256**, 106 (1976)
[14] A Ansari, E Wuest and K Muhlhans, *Nucl. Phys.* **A415**, 215 (1984)
[15] A Ansari, H L Yadav, M Kaushik and U R Jakhar, *Pramana – J. Phys.* **60**, 1171 (2003)
[16] P Ring and P Schuck, *The nuclear many-body problem* (Springer, Berlin, 1980)
[17] M Baranger and K Kumar, *Nucl. Phys.* **A110**, 490 (1968)
[18] A Petrovici, K W Schmid and A Faessler, *Nucl. Phys.* **A665**, 333 (2000)
[19] S G Nilsson *et al*, *Nucl. Phys.* **A131**, 1 (1969)
[20] R Bengtsson, S Frauendorf and F-R May, *At. Data Nucl. Data Tables* **35**, 15 (1986)